ELSEVIER

Contents lists available at ScienceDirect

Journal of Biomechanics

journal homepage: www.elsevier.com/locate/jbiomech





In-vitro stress relaxation response of neonatal peripheral nerves

Tanmay Majmudar ^{a,b}, Sriram Balasubramanian ^a, Rachel Magee ^a, Bernard Gonik ^c, Anita Singh ^{d,*}

- a Drexel University School of Biomedical Engineering, Science, and Health Systems, 3141 Chestnut Street Bossone 718, Philadelphia, PA 19104, United States
- ^b Drexel University College of Medicine, 2900 West Queen Lane, Philadelphia, PA 19129, United States
- c Department of Obstetrics and Gynecology, Wayne State University School of Medicine/Detroit Medical Center, Detroit, MI 48201, United States
- d Department of Biomedical Engineering, Widener University School of Engineering, One University Place, Chester, PA 19013, United States

ARTICLE INFO

Keywords:
Peripheral nerve
Neonate
Stress relaxation
Viscoelastic
Nerve injury

ABSTRACT

Characterizing the viscoelastic behavior of neonatal peripheral nerves is critical in understanding stretch-related peripheral nerve injuries (PNIs) in neonates. This study investigated the in-vitro viscoelastic stress relaxation response of neonatal piglet brachial plexus (BP) and tibial nerves at two different strain levels (10% and 20%) and stress relaxation testing durations (90- and 300-seconds). BP and tibial nerves from 20 neonatal piglets were harvested and pre-stretched to either 10% or 20% strain at a dynamic rate of 100 mm/min to simulate conditions, such as shoulder dystocia, that may lead to stretch-related PNIs in neonates. At constant strain, the reduction in stress was recorded for 90- or 300-seconds. The biomechanical data were then fit to a viscoelastic model to acquire the short- and long-term stress relaxation time-constants. Though no significant differences in the degree of stress relaxation were found between the two tested strain levels after 90 seconds in both nerve types, reduction in stress was moderately greater (p = 0.056) at 10% strain than at 20% for BP after 300 seconds. The reduction in stress was significantly higher in nerves subjected to a 300 second testing duration than 90 second for both strain levels and nerve types. When comparing BP and tibial nerve stress relaxation response, BP nerve relaxed significantly more than tibial at both strain levels after 90 seconds, but no significant differences were observed after 300 seconds. Our results confirm that neonatal peripheral nerve tissue is highly viscoelastic. These novel biomechanical data can be incorporated into finite element and computational models studying neonatal PNIs.

1. Introduction

Peripheral nerve injuries (PNIs) cause considerable disability across the world with a reported incidence between 2 and 2.8% among the trauma population (Noble et al., 1998; Selecki et al., 1982). If plexus and root lesions are also included, the incidence rate is about 5%. Although PNIs are commonly reported in adults and children, they also occur in neonates causing lifelong social and economic burdens (Missios et al., 2014). PNIs in neonates are associated with trauma during complicated childbirth including those observed during neonatal brachial plexus palsy (NBPP) with a worldwide incidence of 1.2 to 2.2 per 1000 live births (Chauhan et al., 2014). NBPP and other neonatal PNIs can result in significant muscle weakness, numbness, and pain and in severe cases, a lifelong loss of motor and sensory function.

One of the challenges faced by clinicians in limiting neonatal PNIs is

due to a poor understanding of the physiological limits of nerve tension. The maximum tension that peripheral nerves can withstand has been mainly reported in adult human and non-human tissue with the biomechanical response primarily depending on the magnitude and rate of lengthening (Kwan et al., 1992; Rydevik et al., 1990; Zapałowicz and Radek, 2005). In a neonatal animal model, Singh et al. (2018) is the only study to report the tensile properties of neonatal peripheral nerves, using piglet brachial plexus and tibial nerve tissue, at different loading rates. Their results suggest that an abrupt traction (studied in the higher stretch rate group) on nerves can result in higher peak stresses thereby making the nerve more susceptible to injury.

The peak stress on a neonatal peripheral nerve, however, may change as a result of its viscoelastic properties. Peripheral nerves, like most biological tissue, undergo stress relaxation – a property of viscoelastic materials that results in a time-dependent reduction in stress after

E-mail address: asingh2@widener.edu (A. Singh).

https://doi.org/10.1016/j.jbiomech.2021.110702

^{*} Corresponding author.at: Department of Biomedical Engineering, Widener University School of Engineering, One University Place, Chester, Pennsylvania 19013, United States.

the material has been stretched and held for a period of time, and is likely dependent upon several factors such as internal fluid pressure (Low et al., 1977), number and distribution of macrostructural elements, such as fascicles (Sunderland and Bradley, 1961), and microstructural elements of the extracellular matrix, such as collagen (Mason and Phillips, 2011; Ushiki and Ide, 1990), elastin (Tassler et al., 1994), and other key proteins (Zilic et al., 2015). Such a situation may arise during complicated shoulder dystocia deliveries, wherein the fetal shoulder impacts the maternal pelvis and the BP is subjected to stretch for prolonged durations that range between 90 and 300 seconds (Beall et al., 1998; Gherman et al., 1998; Hope et al., 1998; Lerner et al., 2011; Spong et al., 1995). Therefore, defining the time-dependent stress relaxation responses of neonatal peripheral nerves, which are currently unavailable, is warranted to better characterize biomechanical injury thresholds of neonatal peripheral nerve tissue. Thus far, data on the stress relaxation responses of peripheral nerves are limited to studies that only utilized adult animal models (Driscoll et al., 2002; Jin et al., 2015; Kendall et al., 1979; Kwan et al., 1992; Piao et al., 2018; Toby et al., 1999; Wall et al., 1991).

Accordingly, this study aims to provide a detailed understanding of the viscoelastic behavior of neonatal peripheral nerves using a piglet animal model. In this study, stress relaxation responses of the neonatal brachial plexus (BP) and tibial nerves were obtained and compared at two different strain levels (10% and 20%) and stress relaxation test durations (90- and 300-seconds).

2. Methods

2.1. Tissue harvest

Eighty BP and 40 tibial nerves harvested from 20 neonatal piglets (3-5 days old) were used in this in-vitro study. Using blunt dissection, the superior and inferior flaps of skin and muscles were released to expose the cervical (C6-8) and thoracic (T1) segments of the BP complex, respectively. The BP complex was then carefully examined to locate the bifurcations of the divisions (M shape) and the segments below the bifurcations were harvested. A total of three non-convergent, chord-nerve segments (including the radial, median and ulnar terminal nerves) could be obtained bilaterally from each animal. Any segments that were surgically compromised were excluded. Harvested tissue were randomly assigned to the study test groups and no segmental comparisons were performed. Using a lateral approach, proximal tibial nerve segments, after bifurcation of the sciatic nerve into tibial and common fibular nerves, were obtained bilaterally from each animal. The freshly harvested nerves were then placed in 1% Bovine Serum Albumin (BSA) for storage until testing, which was performed within two hours of harvest.

2.2. Biomechanical test setup

An ADMET material testing machine (eXpert 7600, ADMET Inc., Norwood, MA) was used to perform stress relaxation testing of the neonatal BP and tibial nerves. As shown in Fig. 1A, the harvested nerves were mounted into the testing setup between the fixed and moving ends using custom designed clamps (detailed in Singh et al. (2006)). Briefly, each custom-built aluminum clamp was L-shaped and consisted of one plexiglass plate with adhesive pads on the clamping site that would secure the tissue during testing while minimizing the stress concentration at the clamping sites. The moving end was equipped with a 200 N load cell that measured the load subjected on the nerve during testing.

2.3. Camera system setup

All tests were recorded using a Basler acA640-120uc high-speed video camera (Basler Inc., Exton, PA) sampling at a rate of 120 fps. The camera was positioned in front of the material testing machine to capture the images of the nerve during testing. These images were later analyzed to determine the strain distribution on the nerve surface, based on positions of two markers placed on the nerve just prior to testing.

2.4. Testing procedures

Harvested neonatal BP and tibial nerves were first divided into two groups (Groups A and B). All samples in Group A were subjected to 90-second stress relaxation tests and those in Group B were subjected to 300-second stress relaxation tests (Fig. 1B). Within each group, samples were further subdivided into two pre-stretch strain levels of 10% and 20% (Fig. 1A). A digital microscope (5X; VHX Microscope, Elmwood Park, NJ) was used to obtain images of harvested BP and tibial nerves before clamping. A 2 mm ruler (Leitz, Ernst-Leitz-Wetzlar GmbH, Germany) at the same magnification was used to measure tissue diameter. The samples were stretched uniaxially at a pre-determined displacement rate of 100 mm/min until the desired strain (10% or 20%) was reached. Stress relaxation data were then recorded for a duration of either 90- or 300-seconds. Subjected strain and displacement rate were controlled by a built-in GaugeSafe software (ADMET Inc., Norwood, MA).

2.5. Viscoelastic constitutive model

The general framework outlined in the Quasi-linear Viscoelastic theory (Fung, 1993) was used to characterize the viscoelastic properties of the neonatal peripheral nerves. According to this theory, stress in a tissue subjected to a certain strain can be expressed as:

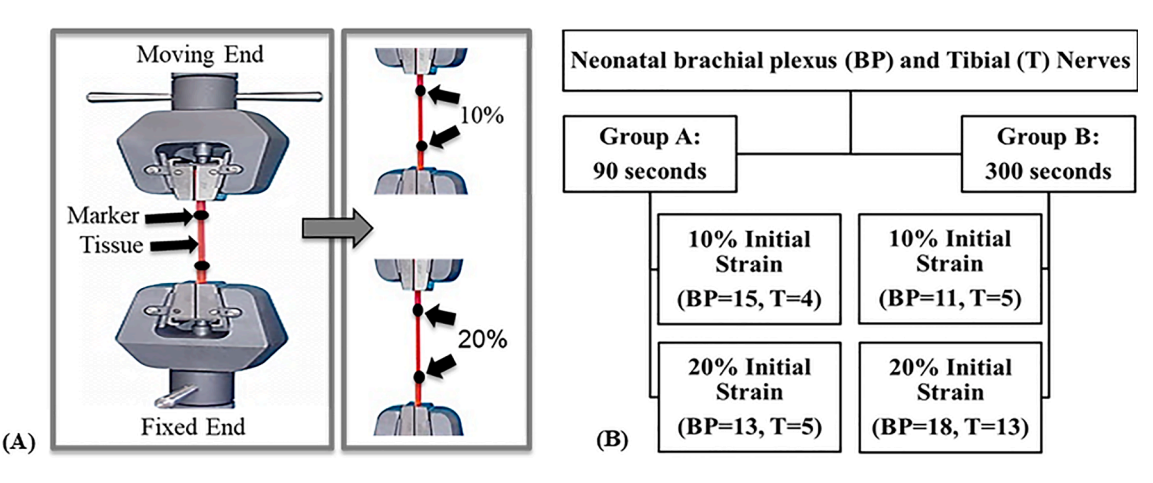


Fig. 1. (A) Schematic of the experimental setup used, including the uniaxial testing machine and (B) diagram detailing the sample size for the various experimental groups.

$$\sigma[\varepsilon(t);t] = G(t) * \sigma^{\varepsilon}(\varepsilon) \tag{1}$$

where $\sigma^e(\varepsilon)$ is the elastic response while G(t) is the reduced relaxation function that represents the time-dependent stress response of the tissue normalized by the stress at the time of the step input of strain [i.e., $t=0^+$, such that $G(t)=\sigma(t)/\sigma(0^+)$ and $G(0^+)=1$]. Although a step change in strain is not practically possible, our experiments were conducted at highly dynamic displacement rates [100 mm/min], and therefore it can be assumed that the stress response measured in this study can be used as a fair approximation of the response to a true step change. Given these conditions, the reduced relaxation function is sufficient to characterize the experimental relaxation data. In the present study, a discrete series of exponentials was used for this function:

$$G(t) = A + Be^{-t/\tau_1} + Ce^{-t/\tau_2}$$
(2)

Eq. (2) represents a generalized Maxwell model. As illustrated in Fig. 2A and 2B, this model consists of three branches, N=2 different Maxwell units in parallel with an elastic spring, and is extensively used to describe the viscoelastic behavior of various biological tissues (Babaei et al., 2016; Faturechi et al., 2019; Toby et al., 1999; Toms et al., 2002; Xu et al., 2008). Previous studies have demonstrated that a model with two Maxwell units provides a reasonably good fit to the experimental data (Babaei et al., 2016). In this model, τ_1 and τ_2 represent the relaxation times describing the short- (initial) and long-term (equilibrium) behavior of the tissue, respectively (Fig. 2C).

2.6. Data analysis

The acquired load, displacement and time data obtained during stress relaxation were utilized for data analysis. Load data were converted to nominal stresses (i.e. load/original cross-sectional area of the sample). The load-time and stress-time curves were then plotted, and the initial peak load and stress values were determined. These stress values $[\sigma(t)]$ were then normalized to produce the reduced relaxation function such that $G(t) = \sigma(t)/\sigma(0^+)$ and G(0) = 1. The reduction in stress at the final time point (either 90- or 300-seconds) was recorded as a percentage of the initial value [G(t)*100]. The reduced relaxation data from the 90- and 300-second stress relaxation tests were combined for each strain level (10% and 20%) and nerve type (BP and tibial). Then Eq. (2) was curve-fitted to this experimental G(t) by determining the five parameters, A, B, C, τ_1 and τ_2 , using nonlinear least-squares regression in MATLAB (MathWorks, Inc., Natick, MA).

2.7. Statistical analysis

Statistical analysis was performed using SPSS software (IBM, Chicago, IL). Values were expressed as mean \pm standard error (mean \pm SEM). Based on data normality determined by Shapiro-Wilk test, parametric testing was performed. Stress relaxation parameters (initial peak load, initial peak stress, and percentage reduction in stress) for each nerve type were compared using a two-way ANOVA with two independent variables – pre-stretch strain level (10% and 20%) and duration (90- and 300–seconds). Subsequent pairwise comparisons were conducted with a Bonferroni correction. Student's t-test was used to assess differences between BP and tibial nerve samples across comparable experimental groups. p < 0.05 was considered significant.

3. Results

Out of the 80 BP and 40 tibial nerves harvested from neonatal piglets, 57 BP and 27 tibial nerves did not slip during testing. Table 1 summarizes the total number, average cross-sectional area, and initial length of BP and tibial nerve samples that were included in the data analysis.

3.1. Stress relaxation response of neonatal Brachial Plexus nerve

The mean initial peak load (N), initial peak stress (MPa) and percentage reduction in stress for neonatal BP nerves are summarized in Table 2. Our results confirm that BP nerve tissue is highly viscoelastic with the reduction in stress being most rapid early on and gradually tailing off (Fig. 3). Of interest is the observation that lower strain tests exhibited a larger reduction in stress at the end of the relaxation behavior. In the 10% strain group, the stress in the BP nerve decreased from the initial peak value by 48.61 \pm 2.51% at 90 seconds and by 70.17 \pm 4.37% at 300 seconds. In the 20% strain group, the stress dropped by 42.65 \pm 1.20% at 90 seconds and by 61.98 \pm 2.97% at 300 seconds. Though no significant differences in the amount of stress relaxation were found between the two tested strain levels after 90 seconds, the reduction in stress was moderately greater (p = 0.056) at 10% strain than at 20% after 300 seconds. Also, the percent reduction in stress was significantly higher in Group B than in Group A at both 10% and 20% strain levels, respectively.

Fig. 3B, D provides a model fit for the stress relaxation response of BP nerve samples maintained at 10% or 20% strain for up to 300 seconds while Table 3 presents the short- and long-term relaxation time-constants derived from this optimized fit. The short-term relaxation time-constant (τ_1) is 3.33% greater in the 10% strain group ($\tau_1 = 8.85$ seconds) than in 20% ($\tau_1 = 8.56$ seconds). Likewise, the long-term

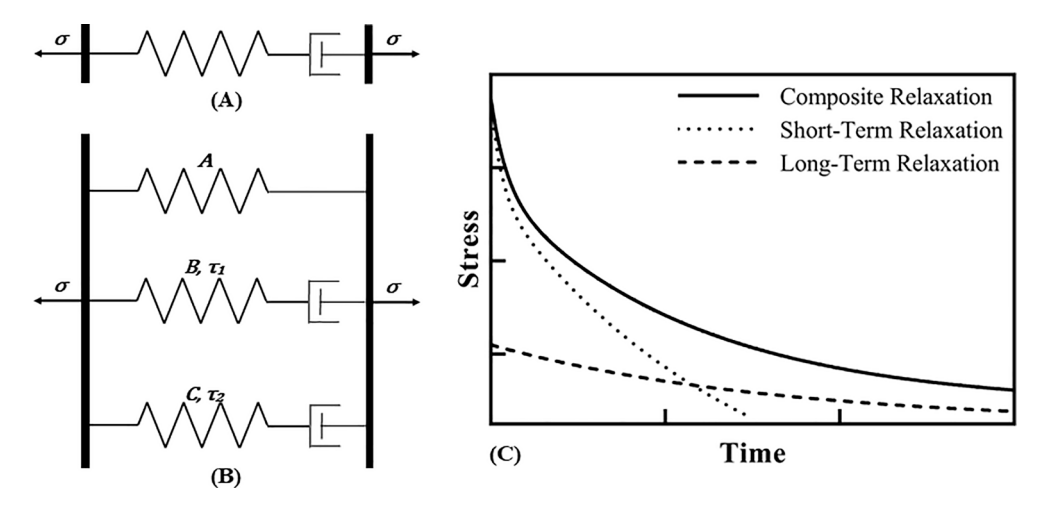


Fig. 2. Schematic of a **(A)** Maxwell unit and **(B)** generalized Maxwell model with N = 2 Maxwell units in parallel with an elastic spring. **(C)** Exemplar stress relaxation curve with short-term, long-term, and composite relaxation behaviors.

Table 1
Summary mean (±SEM) of average cross-sectional area (CSA) (mm²) and initial length (mm) values of Brachial Plexus (BP) and tibial nerve samples when subjected to 90- and 300-second stress relaxation tests under two strain levels (10% and 20%). Tissue slippage at the clamps, indicating a failed experiment, and tissue damage during harvest contributed to the unequal sample sizes in this study.

	Brachial Plexus ($n = 57$)				Tibial $(n=27)$			
Relaxation Time	90 Seconds (G	roup A) (n = 28)	300 Seconds (C	Group B) (n = 29)	90 Seconds (Gr	roup A) (n = 9)	300 Seconds (G	Froup B) (n = 18)
Strain	10%	20%	10%	20%	10%	20%	10%	20%
n	15	13	11	18	4	5	5	13
Average CSA (mm ²)	2.68 ± 0.37	3.39 ± 0.53	2.58 ± 0.30	3.22 ± 0.52	2.72 ± 0.43	2.41 ± 0.67	3.87 ± 1.87	1.80 ± 0.11
Initial Length (mm)	8.27 ± 1.57	7.08 ± 1.02	$\textbf{7.64} \pm \textbf{1.16}$	7.61 ± 1.10	12.50 ± 1.55	12.60 ± 3.44	13.20 ± 2.03	11.93 ± 1.40

Table 2 Summary mean (\pm SEM) of initial peak load (N), initial peak stress (MPa), and reduction in stress (%) values of Brachial Plexus (BP) and tibial nerve samples when subjected to 90- and 300-second stress relaxation duration under two strain levels (10% and 20%). Significant differences in the stress relaxation parameters between the two strain levels are indicated using * (p < 0.1) and ** (p < 0.05) while differences between the two durations are indicated using † (p < 0.1) and †† (p < 0.05). Significant differences between tibial stress relaxation response and the corresponding response in BP are indicated using ## (p < 0.05).

		Brachial Plexus				Tibial			
Relaxation Time	90 Seconds (Group A)		300 Seconds (Group B)		90 Seconds (Group A)		300 Seconds (Group B)		
Strain	10%	20%	10%	20%	10%	20%	10%	20%	
Initial Peak Load (N)	0.58 ± 0.09	$1.62 \pm 0.27^{**}$	0.51 ± 0.12	$1.18\pm0.19^{**,\dagger}$	$1.21 \pm 0.26^{\#\#}$	1.96 ± 0.65	1.13 ± 0.27	$2.13 \pm 0.37^{\#\#}$	
Initial Peak Stress (MPA)	$\textbf{0.32} \pm \textbf{0.07}$	0.45 ± 0.08	0.23 ± 0.05	$0.43\pm0.06^*$	0.45 ± 0.11	0.76 ± 0.20	0.48 ± 0.15	$1.22 \pm 0.20^{**,\#\#}$	
% Reduction in Stress	48.61 ± 2.51	42.65 ± 1.20	$70.17 \pm 4.37^{\dagger\dagger}$	$61.98 \pm 2.97^{*,\dagger\dagger}$	$39.27 \pm 0.54^{\#\#}$	$30.67 \pm 2.97^{\#\#}$	$63.16\pm1.91^{\dagger\dagger}$	$58.26\pm4.72^{\dagger\dagger}$	

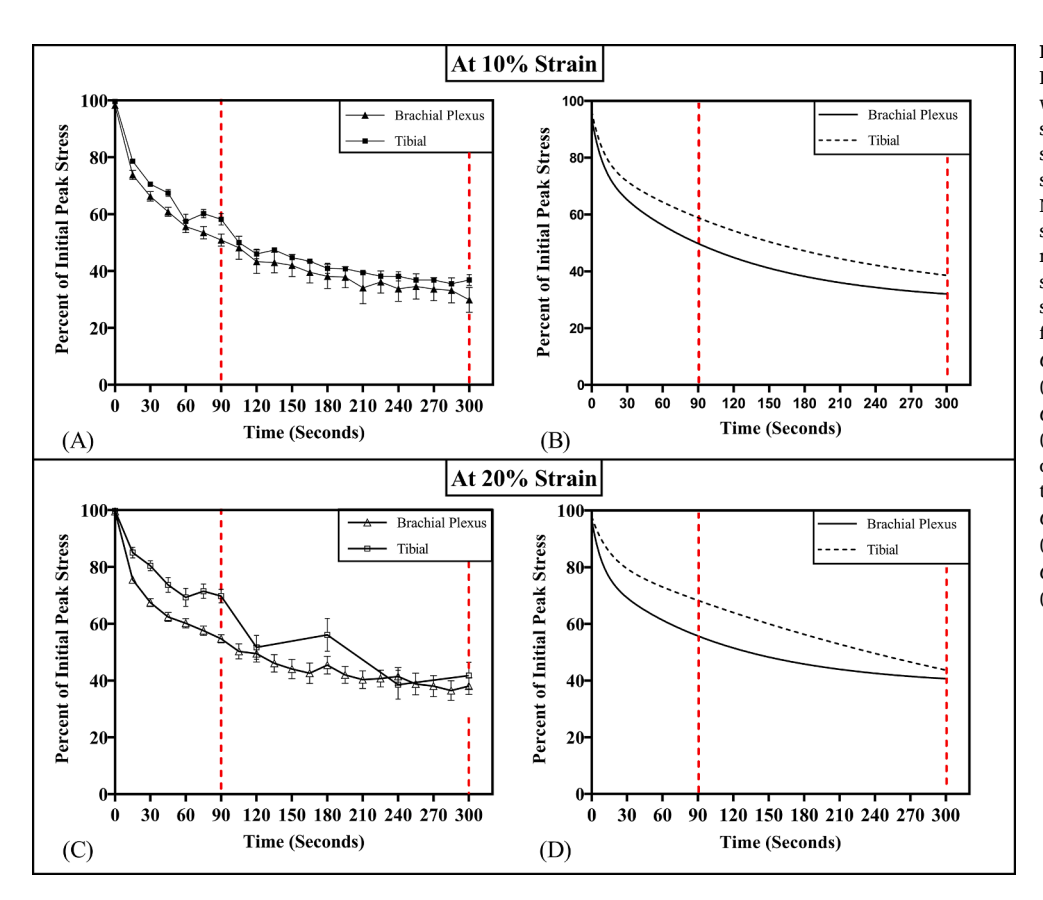


Fig. 3. Stress relaxation response of Brachial Plexus (BP) and tibial nerve samples that were maintained at (A) 10% or (C) 20% strain for 90-300 seconds. Mean (±SEM) stress as a percentage of the initial peak stress is shown (reduced relaxation function). Note: Only data points at 15-second intervals shown for clarity. Model fit for the stress relaxation response of BP and tibial nerve samples stretched to (B) 10% or (D) 20% strain. The optimized reduced relaxation function for the BP 10% data set was $G(t) = 0.29 + 0.18e^{-t/8.85} + 0.47e^{-t/112.62}$ R^2 (Adj. 61%) $G(t) = 0.38 + 0.19e^{-t/8.56} + 0.40e^{-t/109.47}$ (Adj. $R^2 = 73.85\%$) for the 20% dataset. The optimized reduced relaxation function for tibial 10% data set $G(t) = 0.30 + 0.18e^{-t/9.63} + 0.49e^{-t/172.21}$ (Adi. = 95.18%) and $G(t) = 0.03 + 0.15e^{-t/14.12} + 0.80e^{-t/441.90}$ (Adj. $R^2 = 59.68\%$) for the 20% dataset.

relaxation time-constant (au_2) is 2.84% greater in the 10% strain group ($au_2=112.62$ seconds) than in 20% ($au_2=109.47$ seconds).

3.2. Stress relaxation response of neonatal tibial nerve

The mean initial peak load (N), initial peak stress (MPa) and percentage reduction in stress for neonatal tibial nerves are summarized in

Table 2. Similar to neonatal BP nerves, tibial nerves also demonstrated significant viscoelastic stress relaxation with lower strain tests exhibiting a larger reduction in stress at the end of the relaxation behavior (Fig. 3). In the 10% strain group, the stress in tibial nerve decreased from the initial peak value by 39.27 \pm 0.54% at 90 seconds and by 63.16 \pm 1.91% after 300 seconds. In the 20% strain group, the stress dropped by 30.67 \pm 2.97% at 90 seconds and by 58.26 \pm 4.72% at 300 seconds. No

Table 3 Short- (τ_1) and long-term (τ_2) relaxation time-constants for the stress relaxation response of Brachial Plexus (BP) and tibial nerves maintained at 10% or 20% strain for up to 300 seconds.

	Brachia	l Plexus	Til	oial
Strain	10%	20%	10%	20%
τ_1 (seconds)	8.85	8.56	9.63	14.12
τ_2 (seconds)	112.62	109.47	172.21	441.90

statistically significant differences in the amount of stress relaxation were observed between the 10% and 20% strain groups at either duration. Also, the percent reduction in stress was significantly higher in Group B than in Group A at both 10% and 20% strain levels, respectively.

Fig. 3B, D provides a model fit for the stress relaxation response of tibial nerve samples maintained at 10% or 20% strain for up to 300 seconds while Table 3 presents the short- and long-term relaxation time-constants derived from this optimized fit. The short-term relaxation time-constant (τ_1) is 37.81% greater in the 20% strain group (τ_1 = 14.12 seconds) than in 10% (τ_1 = 9.63 seconds), whereas the % difference in the long-term relaxation time-constant (τ_2) is 87.83% with the 20% strain group exhibiting longer times (τ_2 = 441.90 seconds) than 10% (τ_2 = 172.21 seconds).

3.3. Comparing stress relaxation response of neonatal Brachial Plexus and tibial nerve

Differences in the stress relaxation responses between neonatal BP and tibial nerve samples were observed at the two different strain levels (Fig. 3A, C and Table 2) in Group A. At both 10% and 20% strains, the percent reduction in stress in BP nerve (at $10\%-48.61\pm2.51\%$, at $20\%-42.65\pm1.20\%$) was significantly higher than in tibial (at $10\%-39.27\pm0.54\%$, at $20\%-30.67\pm2.97\%$). There was no statistical difference in the amount of stress relaxation between nerve types at either strain in Group B.

Differences in the short- and long-term relaxation time-constants were observed between the nerve types (Fig. 3B, D and Table 3), such that both τ_1 and τ_2 were greater in tibial nerves than in the BP nerves at both strain levels. While τ_1 was greater in the 10% strain group than in 20% for BP nerve, it was smaller in the 10% strain group when compared to 20% for tibial nerve. However, the percent difference in τ_1 between strain levels was greater in tibial nerve (37.81%) than in BP (3.33%). We noticed a similar trend in τ_2 between nerve types – with τ_2 being greater in the 10% strain group than in 20% for BP nerve, and vice-versa for tibial nerves.

4. Discussion

PNIs cause considerable disability and can substantially affect an individual's long-term quality of life (Ciaramitaro et al., 2010). Especially in neonates, PNIs can result in life-long social and economic burdens (Missios et al., 2014). To improve prevention and management strategies for neonatal PNIs, a detailed understanding of the biomechanical response of neonatal peripheral nerve tissue is highly warranted. Ethical limitations in studying human neonatal tissue warrants the use of a large animal model, like piglets, that can serve as a good surrogate to human neonates due to its close anatomical similarities (Gonik et al., 1998). Using piglets, Singh et al. (2018) have reported the biomechanical response of neonatal peripheral nerves under tensile loading at different loading rates. However, the viscoelastic stress relaxation responses were not determined and are currently unavailable. In the present study, we characterized the stress relaxation responses of neonatal piglet BP and tibial nerves under different strain levels and test durations.

Data obtained from the current study provide important insight into the effect of strain on the viscoelastic behavior of neonatal peripheral nerve tissue. Though no significant differences in the amount of stress relaxation were found between the two tested strain levels at 90 seconds in BP nerve, the 10% strain group exhibited a moderately higher (p =0.056) reduction in stress when compared to the 20% strain group at 300 seconds. Although statistically insignificant, this trend was also present in the tibial nerve response. Our findings are similar to those previously reported by Wall et al. (1991) where mature rabbit peripheral nerves stretched to 6% relaxed significantly more than 9% or 12%. The effect of strain as reported in the current study as well as previous studies may be attributed to the initial disposition of nerve fibers within their endoneurial sheaths. At rest, the nerve fibers are known to show an undulated course. Longitudinal stretching up to a certain extent straightens these undulations without altering the structural integrity of the nerve fibers (Clarke and Bearn, 1972; Millesi et al., 1995; Rydevik et al., 1990; Sunderland, 1978). Wall et al. (1992) confirmed this hypothesis by reporting no histological changes in nerves at 6% or 12% strain. Thus, it is possible that the degree of structural deformation contributes to the reduced stress relaxation observed in the higher prestretch strain group (20%) in this study. Further studies using immunohistochemistry or other histological techniques are needed to confirm the postulated changes in nerve structure when subjected to various groups in this study while accounting for nerve structural heterogeneity, such as differences in connective tissue, fat distribution, and axonal waviness, that can influence its viscoelastic response.

Stress relaxation may provide protection to peripheral nerves from prolonged elongation and tensile loads imposed during normal physiological movements (Topp and Boyd, 2006). Previous studies have reported that nerves, within the physiological range of limb motions, may stretch up to 15% without biomechanical deficits (Kwan et al., 1989). The effect of exceeding this strain threshold and stretch duration on nerve stress relaxation response, particularly in neonates, is unknown. A recently published work from our group reported a significant reduction in peak stress at failure in neonatal BP and tibial nerves when subjected to 20% pre-stretch for 300 seconds than 0% pre-stretch (Singh et al., 2021). The current study provides insight into the viscoelastic responses of neonatal peripheral nerve tissue, where BP nerve pre-stretched to 20% strain exhibited reduced stress relaxation than 10% at 300 seconds, which helps understand the reported lower injury threshold in the 20% pre-stretch group at 300 second duration in Singh et al. (2021).

In this study, two different testing durations, 90- and 300-seconds, were chosen. Previous researchers have typically studied long-term stress-relaxation behavior (greater than 30 minutes) in peripheral nerves (Driscoll et al., 2002; Jin et al., 2015; Kendall et al., 1979; Kwan et al., 1992; Piao et al., 2013; Piao et al., 2018; Toby et al., 1999; Wall et al., 1991; Xu et al., 2013). However, to account for nerve stress relaxation responses during traumatic events and birth-related injuries, such as shoulder dystocia, that occur within 90-300 seconds, investigating the short-term nerve stress-relaxation behavior (<300 seconds) is warranted (Beall et al., 1998; Gherman et al., 1998; Hope et al., 1998; Lerner et al., 2011; Spong et al., 1995). Here, we observed significant differences in stress relaxation response between the two time points: the mean reduction in stress was significantly greater after 300 seconds than 90 seconds for both strain levels and nerve types. However, given that previous nerve stress relaxation studies have reported the greatest reduction of stress to occur in the first 10–20 minutes, this finding is not surprising (Brown et al., 1993; Driscoll et al., 2002; Kendall et al., 1979; Kwan et al., 1992; Toby et al., 1999; Wall et al., 1991; Xu et al., 2013).

Information about the stress relaxation response of peripheral nerves is limited and only available from adult tissue. In a comparable study, Wall et al. (1991) reported a 22% reduction in stress after 300 seconds in adult rabbit tibial nerve stretched to 9–12% strain. These values are much lower than those reported in the current study for the 10% strain group (63.16 \pm 1.91%), which confirms that the viscoelastic behavior of peripheral nerves differs between neonatal and adult tissue. Another

study by Driscoll et al. (2002) performed *in-vivo* testing on adult rabbit tibial nerves and reported a mean reduction in stress of < 20% after 300 seconds when stretched to 8.8% or 16.1% strains. These stress relaxation values are lower than those reported in our study, which can be attributed to differences in animal preparation (the current study reported stress relaxation responses in excised nerves) and animal age (current study utilized a neonatal animal model). Future studies investigating the *in-vivo* viscoelastic properties of neonatal peripheral nerves in an animal model are warranted to extend the translational scope of these findings.

In the current study, by fitting the experimentally obtained stress relaxation data to a viscoelastic constitutive model consisting of three springs and two dashpots (the generalized Maxwell model), we determined the short- and long-term relaxation times of neonatal peripheral nerve. To our knowledge, this is the first study to report relaxation times for neonatal peripheral nerve tissue. Results revealed that the long-term relaxation time, τ_2 , is an order of magnitude greater than the short-term relaxation time, τ_1 . This multi-step stress relaxation response likely reflects complexities in neonatal peripheral nerve tissue microarchitecture, such as nonlinearity in extracellular matrix (ECM) biomechanical properties (Mäkelä and Korhonen, 2016; Moreno-Flores et al., 2010) and differences in nerve ultrastructures (Chang et al., 2015), that enable relaxation over vastly different time scales. Nerve tissue viscoelasticity has been minimally studied using constitutive modeling in adult animal models. Gupta et al. (2021) recently quantified the stress relaxation response of adult mouse sciatic nerve using a double-exponential fit. Overall, the short-term relaxation times (\sim 3–5 seconds) were only slightly lower in mouse nerves than that in our study (~8-14 seconds); however, long-term relaxation occurred over a timeframe an order of magnitude greater (~1000-8000 seconds) than the current neonatal model (~100-400 seconds), which could be due to the substantially larger scale of porcine nerves. In addition, differences in cytoskeletal and ECM components between species, which have previously been reported by Zilic et al. (2015), and constitutive modeling approaches could likely explain the variations observed in the reported nerve relaxation times between Gupta et al. (2021) and the current study.

Peripheral nerves exhibit region specific biomechanical behavior such that greater compliance is reported in nerve segments that cross joints than in segments that do not, possibly resulting in differing viscoelastic properties (Phillips et al., 2004). A more recent study also reported sciatic nerve epineurium to have a lower mean density of collagen fibrils than median nerve in both joint and non-joint regions, although the authors did not perform any statistical testing comparing nerve types (Mason and Phillips, 2011). Such regional differences in collagen fibers may influence viscoelastic behavior. Our study further confirms these findings in neonates by reporting differences in viscoelastic stress relaxation response between neonatal BP and tibial nerves. As shown in Table 2 and Fig. 3, neonatal BP nerve relaxed significantly more than tibial after 90 seconds, while no significant differences in stress reduction were found between nerve types after 300 seconds. Viscoelastic constitutive modeling revealed that the long-term stress relaxation constant, τ_2 , is much higher in neonatal tibial than BP nerves, implying that while both BP and tibial nerves may approach a similar level of long-term stress, they do so at different rates. Future histological studies are required to confirms these findings in neonatal peripheral nerve tissue.

This study has a few limitations. Since the displacement rate was matched between the 10% and 20% strain groups, additional stress relaxation might have occurred during the longer loading phase in the 20% strain group. Further work must be undertaken to explore the relative magnitude of this effect on the reported stress relaxation data. The lack of structural assessment using immunohistochemistry and other histological techniques limits the implications of the current findings. Visualizing structural changes in pre-stretched nerve tissue may help explain gross tissue viscoelastic response. Further work investigating structural as well as functional changes in pre-stretched

neonatal nerve is therefore necessary to fully understand the impact of nerve stress relaxation on biomechanical injury thresholds for neonatal peripheral nerves.

In summary, this study is the first to report the *in-vitro* stress relaxation response of neonatal peripheral nerves (BP and tibial) using a piglet animal model at two different strain levels and testing durations. The novel data obtained from this study provide insight into the biomechanical behavior of peripheral nerves in neonates and can be incorporated into finite element simulations or computational models assessing neonatal PNIs.

Declaration of Competing Interest

The authors declare that they have no known competing financial interests or personal relationships that could have appeared to influence the work reported in this paper.

Acknowledgments

The authors would like to thank Virginia Orozco and the late Dr. Maria Delivoria for their assistance with this project. This project was supported by funding from the Eunice Kennedy Shriver National Institute of Child Health and Human Development of the National Institutes of Health under Award Number R15HD093024, and NSF CAREER grant Award #1752513.

References

- Babaei, B., Davarian, A., Pryse, K.M., Elson, E.L., Genin, G.M., 2016. Efficient and optimized identification of generalized Maxwell viscoelastic relaxation spectra. J. Mech. Behav. Biomed. Mater. 55, 32–41.
- Beall, M.H., Spong, C., McKay, J., Ross, M.G., 1998. Objective definition of shoulder dystocia: a prospective evaluation. Am. J. Obstet. Gynecol. 179 (4), 934–937.
- Brown, R., Pedowitz, R., Rydevik, B., Woo, S., Hargens, A., Massie, J., Kwan, M., Garfin, S..R., 1993. Effects of acute graded strain on efferent conduction properties in the rabbit tibial nerve. Clin. Orthop. Relat. Res. (296), 288–294.
- Chang, C.T., Chen, Y.H., Lin, C.C., Ju, M.S., 2015. Finite element modeling of hyperviscoelasticity of peripheral nerve ultrastructures. J. Biomech. 48 (10), 1982–1987.
- Chauhan, S.P., Blackwell, S.B., Ananth, C.V., 2014. Neonatal brachial plexus palsy: Incidence, prevalence, and temporal trends. Semin. Perinatol. 38 (4), 210–218.
- Ciaramitaro, P., Mondelli, M., Logullo, F., Grimaldi, S., Battiston, B., Sard, A., Scarinzi, C., Migliaretti, G., Faccani, G., Cocito, D., 2010. Traumatic peripheral nerve injuries: epidemiological findings, neuropathic pain and quality of life in 158 patients. J. Periph. Nerv. Syst. 15 (2), 120–127.
- Clarke, E., Bearn, J.G., 1972. The spiral nerve bands of Fontana. Brain 95 (1), 1–20.
 Driscoll, P.J., Glasby, M.A., Lawson, G.M., 2002. An in vivo study of peripheral nerves in continuity: biomechanical and physiological responses to elongation. J. Orthop. Res. 20 (2), 370–375.
- Faturechi, R., Hashemi, A., Abolfathi, N., Solouk, A., 2019. Mechanical guidelines on the properties of human healthy arteries in the design and fabrication of vascular grafts: experimental tests and quasi-linear viscoelastic model. Acta. Bioeng. Biomech. 21, 13–21.
- Fung, Y.C., 1993. Biomechanics: Mechanical Properties of Living Tissues. Springer, New York.
- Gherman, R.B., Ouzounian, J.G., Goodwin, T.M., 1998. Obstetric maneuvers for shoulder dystocia and associated fetal morbidity. Am. J. Obstet. Gynecol. 178 (6), 1126–1130.
- Gonik, B., McCormick, E.M., Verweij, B.H., Rossman, K.M., Nigro, M.A., 1998. The timing of congenital brachial plexus injury: A study of electromyography findings in the newborn piglet. Am. J. Obstet. Gynecol. 178 (4), 688–695.
- Gupta, R.S., Berrellez, D., Chhugani, N., Luna Lopez, C., Maldonado, A., Shah, S.B., 2021. Effects of paclitaxel on the viscoelastic properties of mouse sensory nerves. J. Biomech. 115, 110125.
- Hope, P., Breslin, S., Lamont, L., Lucas, A., Martin, D., Moore, I., Pearson, J., Saunders, D., Settatree, R., 1998. Fatal shoulder dystocia: a review of 56 cases reported to the Confidential Enquiry into Stillbirths and Deaths in Infancy. BJOG 105 (12), 1256–1261.
- Jin, H., Yang, Q., Ji, F., Zhang, Y.-J., Zhao, Y., Luo, M., 2015. Human amniotic epithelial cell transplantation for the repair of injured brachial plexus nerve: evaluation of nerve viscoelastic properties. Neural Regen. Res. 10 (2), 260–265.
- Kendall, J.P., Stokes, I.A.F., O'hara, J.P., Dickson, R.A., 1979. Tension and Creep Phenomena in Peripheral Nerve. Acta Orthop. Scand. 50 (6), 721–725.
- Kwan, M.K., Wall, E.J., Massie, J., Garfin, S.R., 1992. Strain, stress and stretch of peripheral nerve Rabbit experiments in vitro and in vivo. Acta Orthop. Scand. 63 (3), 267–272.
- Kwan, M.K., Wall, E.J., Weiss, J.A., Rydevik, B.L., Garfin, S.R., Woo, S.Y., 1989. Analysis of rabbit peripheral nerve: in situ stresses and strains. Biomech. Symp. ASME/AMD. 98, 109–112.

- Lerner, H., Durlacher, K., Smith, S., Hamilton, E., 2011. Relationship between head-to-body delivery interval in shoulder dystocia and neonatal depression. Obstet. Gynecol. 118, 318–322.
- Low, P., Marchand, G., Knox, F., Dyck, P.J., 1977. Measurement of endoneurial fluid pressure with polyethylene matrix capsules. Brain Res. 122 (2), 373–377.
- Mäkelä, J.T.A., Korhonen, R.K., 2016. Highly nonlinear stress-relaxation response of articular cartilage in indentation: Importance of collagen nonlinearity. J. Biomech. 49 (9), 1734–1741.
- Mason, S., Phillips, J.B., 2011. An ultrastructural and biochemical analysis of collagen in rat peripheral nerves: the relationship between fibril diameter and mechanical properties. J. Periph. Nerv. Syst. 16 (3), 261–269.
- Millesi, H., Zoch, G., Reihsner, R., 1995. Mechanical properties of peripheral nerves. Clin. Orthop. Relat. Res. (314), 76–83.
- Missios, S., Bekelis, K., Spinner, R.J., 2014. Traumatic peripheral nerve injuries in children: epidemiology and socioeconomics. J. Neurosurg. Pediatr. 14 (6), 688–694.
- Moreno-Flores, S., Benitez, R., Vivanco, M.D., Toca-Herrera, J.L., 2010. Stress relaxation microscopy: Imaging local stress in cells. J. Biomech. 43 (2), 349–354.
- Noble, J., Munro, C.A., Prasad, V.S.S.V., Midha, R., 1998. Analysis of upper and lower extremity peripheral nerve injuries in a population of patients with multiple injuries. J. Trauma. 45 (1), 116–122.
- Phillips, J.B., Smit, X., Zoysa, N.D., Afoke, A., Brown, R.A., 2004. Peripheral nerves in the rat exhibit localized heterogeneity of tensile properties during limb movement. J. Physiol. 557, 879–887.
- Piao, C., Li, P., Liu, G., Yang, K., 2013. Viscoelasticity of repaired sciatic nerve by poly (lactic-co-glycolic acid) tubes. Neural Regen. Res. 8 (33), 3131–3138.
- Piao, C., Li, Z., Ding, J., Kong, D., 2018. Analysis of BMSCs-intervened viscoelasticity of sciatic nerve in rats with chronic alcoholic intoxication. Acta Cir. Bras. 33 (10), 935–944.
- Rydevik, B.L., Kwan, M.K., Myers, R.R., Brown, R.A., Triggs, K.J., Woo, S.Y., Garfin, S.R., 1990. An in vitro mechanical and histological study of acute stretching on rabbit tibial nerve. J. Orthop. Res. 8 (5), 694–701.
- Selecki, B.R., Ring, I.T., Simpson, D.A., Vanderfield, G.K., Sewell, M.F., 1982. Trauma To The Central And Peripheral Nervous Systems Part II: A Statistical Profile Of Surgical Treatment New South Wales 1977. Aust. N Z J Surg. 52 (2), 111–116.
- Singh, A., Lu, Y., Chen, C., Cavanaugh, M.J., 2006. Mechanical properties of spinal nerve roots subjected to tension at different strain rates. J. Biomech. 39, 1669–1676.
- Singh, A., Majmudar, T., Magee, R., Balasubramanian, S., Gonik, B., 2021. Effects of Prestretch on Neonatal Peripheral Nerve: An In-Vitro Study. J. Brachial. Plex. Peripher. Nerve Inj. [Available Online].

- Singh, A., Shaji, S., Delivoria-Papadopoulos, M., Balasubramanian, S., 2018. Biomechanical Responses of Neonatal Brachial Plexus to Mechanical Stretch. J. Brachial. Plex. Peripher. Nerve Inj. 13 (01), e8–e14.
- Spong, C., Beall, M., Rodrigues, D., Ross, M., 1995. An objective definition of shoulder dystocia: prolonged head-to-body delivery intervals and/or the use of ancillary obstetric maneuvers. Obstet. Gynecol. 86 (3), 433–436.
- Sunderland, S., 1978. Nerves and Nerve Injuries, 2nd ed. Williams and Wilkins, Baltimore.
- Sunderland, S., Bradley, K.C., 1961. Stress-strain phenomena in human peripheral nerve trunks. Brain 84 (1), 102–119.
- Tassler, P.L., Dellon, A.L., Canoun, C., 1994. Identification of Elastic Fibres in the Peripheral Nerve. J. Hand Surg. 19 (1), 48–54.
- Toby, E.B., Rotramel, J., Jayaraman, G., Struthers, A., 1999. Changes in the Stress Relaxation Properties of Peripheral Nerves After Transection. J. Hand Surg. Am. 24 (4), 694–699.
- Toms, S.R., Dakin, G.J., Lemons, J.E., Eberhardt, A.W., 2002. Quasi-linear viscoelastic behavior of the human periodontal ligament. J. Biomech. 35 (10), 1411–1415.
- Topp, K.S., Boyd, B.S., 2006. Structure and Biomechanics of Peripheral Nerves: Nerve Responses to Physical Stresses and Implications for Physical Therapist Practice. Phys. Ther. 86, 92–109.
- Ushiki, T., Ide, C., 1990. Three-dimensional organization of the collagen fibrils in the rat sciatic nerve as revealed by transmission- and scanning electron microscopy. Cell Tissue Res. 260 (1), 175–184.
- Wall, E.J., Kwan, M.K., Rydevik, B.L., Woo, S.L-Y., Garfin, S.R., 1991. Stress relaxation of a peripheral nerve. J. Hand Surg. Am. 16 (5), 859–863.
- Wall, E.J., Massie, J.B., Kwan, M.K., Rydevik, B.L., Myers, R.R., Garfin, 1992.
 Experimental stretch neuropathy. Changes in nerve conduction under tension.
 J. Bone Joint Surg. Br. 74-B (1), 126–129.
- Xu, D., Zhao, C., Ma, H., Wei, J., Li, D., 2013. Comparison of viscoelasticity between normal human sciatic nerve and amniotic membrane. Neural Regen. Res. 8, 1269–1275.
- Xu, F., Seffen, K., Lu, T., 2008. A Quasi-Linear Viscoelastic Model for Skin Tissue. Theor. Exp. Asp. Continuum. Mech.
- Zapałowicz, K., Radek, A., 2005. Experimental investigations of traction injury of the brachial plexus. Model and results. Ann. Acad. Med. Stetin. 51, 11–14.
- Zilic, L., Garner, P.E., Yu, T., Roman, S., Haycock, J.W., Wilshaw, S.P., 2015. An anatomical study of porcine peripheral nerve and its potential use in nerve tissue engineering. J. Anat. 227 (3), 302–314.